Ridge Structure Enhancement for Optical Coherence Tomography Latent Fingerprint Images

Sboniso Sifiso Mgaga
Secure Identity Systems
Council for Scientific and Industrial Research
Pretoria, South Africa
SMgaga@csir.co.za

Nontokozo Portia Khanyile
Secure Identity Systems
ICSC, CSIR
Pretoria, South Africa
PKhanyile@csir.co.za

Ntombizodwa Thwala
Governance, Privacy & Trust
Council for Scientific and Industrial Research
Pretoria, South Africa
NThwala1@csir.co.za

Kedimotse Baruni
Secure Identity Systems
Council for Scientific and Industrial Research
Pretoria, South Africa
KBaruni@csir.co.za

Nthabiseng Mokoena
Secure Identity System
ICSC, CSIR
Pretoria, South Africa
NMokoena1@csir.co.za

Cynthia Sthembile Ntshangase
Secure Identity Systems
Council for Scientific and Industrial Research
Pretoria, South Africa
SMlambo@csir.co.za

***Abstract*—This paper proposes a method to improve the ridge structure in latent fingerprint images captured through optical coherence tomography (OCT). Friction ridges, which compose fingerprints, play a crucial role in forensic investigations as they enable individual identification. Unfortunately, latent fingerprint images frequently possess low quality, leading to subpar performance in automatic fingerprint identification systems (AFIS). To address this issue, a technique that combines wavelet-based denoising, morphological segmentation and ridge structure enhancement is presented. The experimental results, measured by the orientation certainty level (OCL), demonstrate the effectiveness of the proposed enhancement method in noise reduction while preserving accurate values in areas with high curvature.**

***Index Terms*—Ridge enhancement, OCT, latent fingerprints, contactless, segmentation**

I. Introduction

Fingerprints consist of unique patterns known as friction ridges, making them the most widely used and popular biometric identifier due to their universality and distinctiveness [16]. In the field of forensics, fingerprints play a crucial role in individual identification. However, fingerprint images often suffer from low quality, leading to subpar performance in Automatic Fingerprint Identification Systems (AFIS).

In [15], the authors introduced a speckle-noise removal technique based on adaptive thresholding [6] and the NormalShrink method [14] to address this issue. To evaluate the effectiveness of their proposed technique, they utilized performance metrics such as peak signal-to-noise ratio, signal-to-noise ratio, mean squared error, root mean square error and structural similarity index measure. Through experimental results, it was demonstrated that the method presented in [15] outperformed other approaches including adaptive thresholding, NormalShrink, VisuShrink, SUREShrink, and BayesShrink.

Building upon the work conducted in [15], this paper expands the enhancement of latent fingerprint images obtained through Optical Coherence Tomography (OCT). In addition to the wavelet-based denoising, we propose morphological segmentation and ridge structure enhancement as supplementary techniques, as depicted in Fig. 1 . To elaborate, after applying VisuShrink, BayesShrink, SUREShrink, NormalShrink, adaptive thresholding, and / or the technique from [15] to OCT latent fingerprint images, we perform image segmentation and ridge structure enhancement. This includes processes such as normalization, ridge orientation field estimation, ridge frequency estimation, ridge filtering, and binarization. The ridge structure enhancement aims to improve the texture and contrast of ridges and valleys in the fingerprint image.

Council for Scientific and Industrial Research.

II. Segmentation

Image segmentation is the process of segregating a digital image into multiple fragments of group pixels [18]. The aim of segmenting the image is to change the presentation of an image into something that is easier to analyse. In this work, morphological segmentation technique described in [5] was used.

A. Morphological operations

In image processing, morphology refers to the set of image processing operations that process shape-based images. The value of each pixel in the output image in a morphological operation is based on a comparison of the corresponding pixel in the input image with that of the neighbours. Morphological operation is a non-linear shape-oriented technique that uses a 3D Structural Element (SE). A SE is a matrix used to spot the image pixel being processed and defines the neighbourhood used in the processing of each pixel in an image. The SE matrix is made up of 1's and 0's that can have any size and shape. The neighbourhood is defined by the pixels with the value of 1 . In an image, isolated foregrounds may be removed by erosion while narrow regions are thickened by dilation operation. Dilation and erosion are the two most

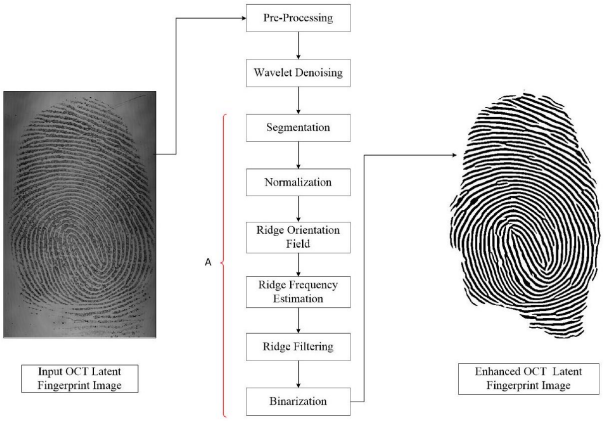

Fig. 1: OCT latent fingerprint images enhancement procedure. Segmentation and ridge structure enhancement are represented by 'A'.

critical morphological operations. Erosion removes pixels on object boundaries, while dilation adds pixels to object boundaries [19]. When performing morphological operations, the SE is positioned in the surface of the image at all possible locations and is compared with the corresponding pixels of the neighbourhoods [5]. Formally, the erosion of an image I by SE Z is denoted as $I \Theta Z$. The dilation of an image I by SE Z is denoted as $I \oplus Z$.

B. Segmentation Process

- For a given grayscale fingerprint image, calculate the range, R, over a block of size $w \times w$ to highlight the ridges.
- Set an appropriate threshold level for each block size (16×16), the adaptive threshold described in [6] was used.
- Use the disk-shaped SE of radius r to apply the morphological closing operation.
- Extract the foreground, with the operation $I - I \Theta Z$, where Z is a disk-shaped SE, of radius $r = 3$. Retain only the contour with the largest perimeter. Since fingerprints are curved in nature a disk-shaped SE was chosen for the closing operation. Normally, the separation between ridges varies between $3 - 18$ pixels, so a disk with a radius of $(r = 6)$ is adequate to highlight the ridges and to eliminate the spurs.

C. Contour smoothing

To achieve better results, a post-processing step is necessary. The contour filtering method in a complex Fourier transform domain proposed in [7] is used. The steps of the post-processing are as follows:

- Find the contour of the segmented binary fingerprint image.
- For every point on the contour, find the coordinate (i, j). Then, find (x_c, y_c) the centroid of the boundary.
- Convert the $(x - x_c, y - y_c)$ to polar coordinates (r, θ).
- Using the complex Fourier series, expand r.

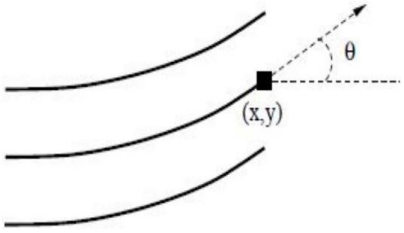

Fig. 2: Orientation field of a ridge at pixel (i, j).

III. Ridge Structure Enhancement

A. Normalization

In image processing, normalization is the global operation that changes the pixel intensity to fit a certain desired range. The variations on an image may be caused by dust on the finger, dryness of the skin, irregular pressure on the scanner, which cause the captured images to vary. Normalization reduces the effect of the above factors, including those that occur during the image acquisition stage and also minimizes the chance of valid features being rejected. A grayscale image I, is defined as:

$$I = \{(i, j, x_{ij}) \mid 0 \leq i \leq N - 1 \wedge 0 \leq j \leq M - 1 \wedge 0 \leq x_{ij} \leq R - 1\} \quad (1)$$

where (i, j, x_{ij}) is the pixel of the image I, with (i, j) being the position of the pixel and x_{ij} its intensity value. For simplicity, the pixel (i, j, x_{ij}) is denoted as (i, j), which is adopted in this paper. The normalized grayscale image G is defined as [9]:

$$G(i,j) = \begin{cases} M_0 + \sqrt{\frac{\sigma_0^2 (I(i,j) - M)^2}{\sigma^2}}, & \text{if } I(i,j) > M \\ M_0 - \sqrt{\frac{\sigma_0^2 (I(i,j) - M)^2}{\sigma^2}}, & \text{Otherwise} \end{cases} \quad (2)$$

where M and σ^2 represent the estimated mean and variance of image I, respectively. The mean M_0 and variance σ_0^2 are the desired mean and variance values of $G(i, j)$, respectively.

IV. Ridge Orientation Field

Orientation field estimation is a technique used to enhance the global features of fingerprint images. It describes the local orientation of the ridge-valley structure at each point of a fingerprint image [22]. The orientation field of an image is constructed from directional vectors estimated from the normalized image. Figure 2 shows the ridge orientation at pixel (i, j). Orientation of an image can be used in singular-point detection, fingerprint image enhancement and classification [2], [13], [20].

Different techniques for estimating orientation have been developed [4], [9], [12], [21], [22]. The gradient-based technique appears to be the most common used method [4], [9], [21]. This research work adopts the same approach in [9] to calculate the gradient of the normalized image. The computed gradient is then used in the least square algorithm. In the least square-algorithm, ridge orientation estimation is based

on the gradient (G_x, G_y) relationship between neighbouring pixels. Given a normalized image, $G(i,j)$, the gradient based orientation field estimation comprises the following steps [2], [13], [20], [21]:

- Divide the normalized OCT latent fingerprint image G into $w \times w$ non-overlapping blocks.
- At each pixel of the fingerprint image, $I(i,j)$, compute the gradients G_x and G_y by using the Scharr operator [8]. Each pixel of the $w \times w$ is convolved by using vertical and horizontal Scharr kernels S_y and S_x, respectively, in order to find the direction of the maximum intensity fluctuation.

$$S_x = \begin{bmatrix} -3 & 0 & +3 \\ -10 & 0 & +10 \\ -3 & 0 & +3 \end{bmatrix}, \quad S_y = \begin{bmatrix} -3 & -10 & -3 \\ 0 & 0 & 0 \\ +3 & +10 & +3 \end{bmatrix}$$

- If $G_x = G_y$ then add ± 1 randomly to one of the gradients i.e G_x or G_y. Also for $G_x = 0$ or $G_y = 0$ add ± 1 randomly to G_x or G_y.
- Evaluate the local orientation in $w \times w$ blocks centred at pixel (x, y) by using the following equations:

$$V_y(i,j) = \sum_{u=i-\frac{w}{2}}^{i+\frac{w}{2}} \sum_{v=j-\frac{w}{2}}^{j+\frac{w}{2}} 2G_x(u,v)G_y(u,v) \tag{3}$$

$$V_x(i,j) = \sum_{u=i-\frac{w}{2}}^{i+\frac{w}{2}} \sum_{v=j-\frac{w}{2}}^{j+\frac{w}{2}} G_x^2(u,v) - G_y^2(u,v) \tag{4}$$

$$\phi_x(x,y) = \frac{1}{2} \arctan\left(\frac{V_x(i,j)}{V_y(i,j)}\right) \tag{5}$$

$$\theta_{gr}(i,jy) = \phi_x(i,j) + k\pi \tag{6}$$

where:

$$k = \begin{cases} \frac{1}{2}, & \text{if } (\phi(x,y) < 0 \wedge V_x(i,j) < 0) \vee (\phi(i,j) \geq 0 \wedge V_x(i,j) > 0 \\ 1, & \text{if } (\phi(i,j) < 0 \wedge V_x(i,j) \geq 0) \\ 0, & \text{if } \phi(i,j) \geq 0 \wedge V_x(i,j) \leq 0 \end{cases} \tag{7}$$

- The estimated local ridge orientation, $\theta_{gr}(i,j)$, may not always be reliable due to noise, corrupted ridge-valley structure and minutia points on the fingerprint image. A low-pass filter is applied to reduce the effects of noise. In order to use the low-pass filter successfully, the orientation of an image must be continuous. An orientation of an image is transformed into continuous vector by using equations (8) and (9).

$$\phi_x(i,j) = \cos 2\left(\theta_{gr}(i,j)\right) \tag{8}$$

and

$$\phi_y(i,j) = \cos 2\left(\theta_{gr}(i,j)\right) \tag{9}$$

where ϕ_x and ϕ_y are the x and y components of the vector field, respectively. The computed vector field is then used for low-pass filtering as follows:

$$\phi'_x(i,j) = \sum_{u_x=-\frac{w_\phi}{2}}^{\frac{w_\phi}{2}} \sum_{v_x=-\frac{w_\phi}{2}}^{\frac{w_\phi}{2}} W(u_x,v_x)\,\phi_x(i-wu_x, j-wv_x) \tag{10}$$

and

$$\phi'_y(i,j) = \sum_{u_y=-\frac{w_\phi}{2}}^{\frac{w_\phi}{2}} \sum_{v_y=-\frac{w_\phi}{2}}^{\frac{w_\phi}{2}} W(u_y,v_y)\,\phi_y(i-wu_y, j-wv_y) \tag{11}$$

where $w_\phi \times w_\phi$ is the filter size and W is the low-pass filter with a unit integral.

- The local ridge orientation of pixel (i,j) is then calculated by using

$$\Theta(i,j) = \frac{1}{2} \arctan\left(\frac{\phi'_y(i,j)}{\phi'_x(i,j)}\right) + k\pi \tag{12}$$

- The reliability of the orientation $\Theta(i,j)$ of the block is estimated by using a metric referred to as coherence [10]. The coherence of the block is computed as,

$$\mathrm{Coh}_B = \frac{\left|\sum_{i=1}^{w}\sum_{j=1}^{w} V_x(i,j), V_y(i,j)\right|}{\sum_{i=1}^{w}\sum_{j=1}^{w} |V_x(i,j), V_y(i,j)|} \tag{13}$$

V. Ridge Frequency Estimation

The distance from a given ridge to its adjacent ridges is referred to as inter-ridge distance [1]. The ridge frequency is the reciprocal of inter-ridge distance, indicating the number of ridges within a unit length of an image. The fingerprint ridge frequency describes the local distance between ridges at each point of the fingerprint image. To estimate a frequency of an image successfully, a normalized image which is divided into $w \times w$ is required. The algorithm used in [9] for estimating frequency calculates an oriented window of size $w \times w$ for each block centred at (i,j) as follows [9]:

- Divide OCT latent fingerprint image G into blocks of size $w \times w$.
- Calculate an oriented window of size $I \times w$, specified in the ridge coordinate system [9], for each block centred at (i,j)
- For each block centred at (i,j), calculate the x-signature, $X[0], X[1], \ldots, X[I-1]$ of the ridges and valleys within the orientated window, where

$$X[k] = \frac{1}{w} \sum_{d=0}^{w-1} G(u,v), k = 0,1,2,\ldots,I-1 \tag{14}$$

$$u = i + \left(d - \frac{w}{2}\right)\cos\Theta(i,j) + \left(k - \frac{1}{2}\right)\sin\Theta(i,j) \tag{15}$$

$$v = i + \left(d - \frac{w}{2}\right)\sin\Theta(i,j) + \left(k - \frac{1}{2}\right)\cos\Theta(i,j) \tag{16}$$

- Let $\eta(i,j)$ represent the mean of the pixels between two consecutive peaks in the x-signature, then the frequency, $\mu(i,j)$, is calculated as:

$$\mu(i,j) = \frac{1}{\eta(i,j)} \tag{17}$$

If the x-signature does not have consecutive peaks, the frequency is given a value of -1 to distinguish it from the valid frequency values.

- A latent fingerprint image may be affected by three factors: the area of the fingerprint that is captured, the size of the image and the resolution. These factors are related to one another as follows [24]:

$$H_{\text{height}} = \frac{h}{r} \times 25.4 \tag{18}$$

$$W_{width} = \frac{w}{r} \times 25.4 \tag{19}$$

where h and w denote the height and width of the image, r represents the resolution in dots per inch (dpi), and $(H_{height}$ & $W_{width})$ denotes the height and width of the captured area. The OCT latent fingerprint images are captured at different resolutions and have different widths and heights. Therefore, for each captured fingerprint image the value of the frequency of the ridges and valleys in a local neighbourhood lies in a different range. For example, an image of 640 by 480 pixels and 661 dpi has the range of $(24.59, 18.44)$ millimetres. Therefore, any estimated frequency value that is out of this range is assigned a numeric value -1 to show that a frequency obtained is invalid.

- A well defined sinusoidal-shaped wave is not formed when the blocks in which ridges and valleys occur are corrupted. Then these corrupted blocks are interpolated from the frequency of the neighbouring blocks which have well-defined frequencies. The blocks are interpolated as follows:
(a) For each block centred at (i,j) :

$$\Omega'(i,j) = \begin{cases} \Omega(i,j), & \text{if } \Omega(i,j) \neq -1 \\ \frac{\sum_{u=-\frac{w_\Omega}{2}}^{\frac{w_l}{2}} \sum_{v=-\frac{w_\Omega}{2}}^{\frac{w_l}{2}} W_g(u,v)\mu(\Omega(i-wu,j-wv))}{\sum_{u=-\frac{w_\Omega}{2}}^{\frac{w_l}{2}} \sum_{v=-\frac{w_\Omega}{2}}^{2} W_g(u,v)\delta(\Omega(i-wu,j-wv)+1)}, & \text{Otherwise} \end{cases} \tag{20}$$

where

$$\mu(x) = \begin{cases} 0, & \text{if } x \leq 0 \\ x, & \text{Otherwise} \end{cases}$$

$$\delta(x) = \begin{cases} 0, & \text{if } x \leq 0 \\ 1, & \text{Otherwise} \end{cases}$$

where W_g is a discrete Gaussian kernel with mean $= 0$ and variance $= 9$, and $w_\Omega = 7$ is the size of the kernel.
(b) Swap Ω&Ω' and go to step (a) if there is one block with a frequency value of -1.

- To remove outliers in $F(i,j)$, a low-pass filter is used:

$$F(i,j) = \sum_{u=-\frac{w_l}{2}}^{\frac{w_l}{2}} \sum_{v=-\frac{w_\Omega}{2}}^{\frac{w_l}{2}} W_l(u,v)\Omega'(i-wu, j-wv) \tag{21}$$

W_l is a 2D low-pass filter with unit integral and $w_l = 7$ is the size of the filter.

VI. Ridge Filtering

Gabor filtering [3] is a linear filter that can be used to analyse image texture. This filter is a sinusoidal plane wave which uses both frequency and orientation properties of the image. In fingerprint images, it is used to solve broken ridges and smudges. In this work, the even-symmetric Gabor filter has been used [17].

$$h(x,y:\alpha,f) = \exp\left\{-\frac{1}{2}\left[\frac{x_\alpha^2}{\delta_x^2} + \frac{y_\alpha^2}{\delta_y^2}\right]\right\} \cos(2\pi f x_\alpha) \tag{22}$$

$$x_\alpha = x\cos\alpha + y\sin\alpha, \tag{23}$$

$$x_\alpha = y\cos\alpha - x\cos\alpha \tag{24}$$

where α is the orientation of the Gabor filter, f is the frequency of a sinusoidal plane wave and δ_x and δ_y are the space constants of the Gaussian envelope along the x and y axes, respectively. In order for the Gabor filter to enhance an image, the filter has to be convolved with the pixel (i,j). The corresponding orientation value $(\Theta(i,j))$ and the frequency value $F(i,j)$ are required. This is defined mathematically as

$$E(i,j) = \sum_{u=-\frac{w_x}{2}}^{\frac{w_x}{2}} \sum_{v=-\frac{w_y}{2}}^{\frac{w_y}{2}} G(u,v;\Theta(i,j),F(i,j)N(i-u,j-v)) \tag{25}$$

where $N(i-u,j-v)$ is the normalized fingerprint image, $F(i,j)$ is the ridge frequency image, $\Theta(i,j)$ is the orientation image and w_x&w_y are the width and height of the Gabor filter mask, respectively. The problem with the original Hong *et al.* [9] enhancement technique is the fact that the values of the standard deviation δ_x and δ_y are fixed to the value 4 . Using the fixed values forces the bandwidth of the filter to be constant; this means that the variations that occur in the value of the ridge frequency are not taken into account. Therefore, for fingerprint images that exhibit significant variation in the frequency value, enhancement artefacts will occur. Therefore, in this work, we adopt the solution proposed in [17]. Instead of using fixed values Thai *et al.* [17] used the standard deviation values δ_x and δ_y as the function of ridge frequency, defined as [11], [17]:

$$\delta_x = k_x F(i,j), \tag{26}$$

$$\delta_y = k_y F(i,j), \tag{27}$$

where k_x is a constant variable for δ_x, k_y is a constant variable for δ_y and F is the ridge frequency image. Furthermore Thai et al. set the filter size to depend on standard deviation parameters to accommodate Gabor wave-forms of different bandwidth sizes.

$$w_x = 6\delta_x \tag{28}$$

$$w_y = 6\delta_y \tag{29}$$

where δ_y and δ_x are the standard deviations of the Gaussian envelope along the x and y axes, the width and height of the Gabor filter mask are represented by w_x and w_y, respectively.

VII. OCT Latent Fingerprints

In this study we utilized a database obtained through a cutting-edge spectral-domain Optical Coherence Tomography (SD-OCT) system.

The SD-OCT system employed a super-luminescent diode with a central wavelength of 930 nm, offering excellent precision. It boasted an average power output of 10 mW, ensuring optimal imaging capabilities. With an impressive imaging depth of 2.9 mm and a scanning speed of 100 kHz, the SD-OCT system provided us with a robust platform for our research endeavors.

The study encompassed an analysis of a database consisting of 270 latent fingerprint images, carefully constructed through a rigorous process. The database was generated by engaging the participation of 5 individuals and encompassed six distinct surfaces, including glass, stainless steel knife, brass door knob, plastic, mirror, and smartphone screen. From each participant, we selected three fingers, namely the index finger, middle finger, and thumb. To ensure comprehensiveness, we captured three impressions of each finger. As a result, our database encompassed a total of $5 \times 6 \times 3 \times 3 = 270$ latent fingerprint images, representing a diverse and rich collection of data for our study.

VIII. Quality Assessment

OCL measures the energy concentration along the dominant direction of the ridges. The OCL quality estimation metric as described in [23] is used to estimate the OCT latent fingerprint images quality. The OCL values for each wavelet denoising technique are measured at a specific decomposition level and with a certain filter.

IX. Experimental Results

In Fig. 3, the entire proposed enhancement technique is depicted. Figures 4 and 5 illustrate the OCL values of OCT latent fingerprint images after segmentation and ridge structure enhancement, respectively. The numbers on x-axis represents the wavelet denoising techniques as investigated in [15], i.e. 1-VisuShrink, 2-BayesShrink, 3-SUREShrink, 4-NormalShrink, 5-adaptive threshold and 6-technique proposed by Mgaga *et al.* [15].

X. Discussion

A. Segmentation

- The analysis of Figures 4a, 4b, 4c and 4d, specifically at haar level 1, reveals that BayesShrink exhibits a superior OCL value. However, at haar levels 2 and 4, SUREShrink emerges as the preferred choice, demonstrating its desirability in those decomposition levels. Notably, the proposed technique demonstrates its effectiveness particularly at haar level 4 of decomposition. This analysis showcases the performance characteristics of different methods across various haar decomposition levels, highlighting their respective strengths and indicating the optimal application of the proposed technique at haar level 4.
- Figure 4d (db2 wavelet filter) demonstrates that the proposed technique yields better OCL values at level 1 and level 3. Conversely, BayesShrink showcases its effectiveness at level 2 and level 4. This analysis highlights the varying strengths of these techniques across different levels of wavelet decomposition, emphasizing the optimal performance of the proposed technique at level 1 and level 3, while recognizing the efficacy of BayesShrink at level 2 and level 4.
- In Fig. 4c (sym4 wavelet filter), the proposed technique is superior at level 1, VisuShrink is effective at level $2\&4$, and BayesShrink is better at level 4.
- In Fig. 4d (bior2.6 wavelet filter), the effectiveness of different techniques varies across different levels of wavelet decomposition. At level 1, the proposed technique demonstrates its effectiveness. On the other hand, at level 2, the adaptive threshold method outperforms others. At level 3, BayesShrink emerges as the desirable choice, while at level 4, VisuShrink showcases its effectiveness. This analysis highlights the strengths and suitability of different techniques at various levels of wavelet decomposition, providing valuable insights for selecting the optimal approach based on specific decomposition requirements.

B. Ridge Structure Enhancement

- Figure 5b (db2 wavelet filter) demonstrates the exceptional performance of the SUREShrink technique, achieving an impressive OCL value of 86.3231 at level 4 wavelet decomposition. On the other hand, as shown in Fig. 5c, VisuShrink exhibits superior performance at level 2. Notably, in Fig. 5a, the adaptive threshold method dominates the results at level 1 decomposition. This analysis highlights the effectiveness of different techniques across varying levels of wavelet decomposition, showcasing their respective strengths and optimal performance in enhancing the ridge structure of latent fingerprint images.
- Figure 5d (bior2.6 wavelet filter) exhibits the optimal performance of the proposed method at level 1, achieving an impressive OCL value of 86.3884. Throughout this

(a) (b)

(c) (d)

Fig. 3: Proposed enhancement images from (a) Original image, (b) denoised image [15], (c) segmented image up to (d) enhanced image

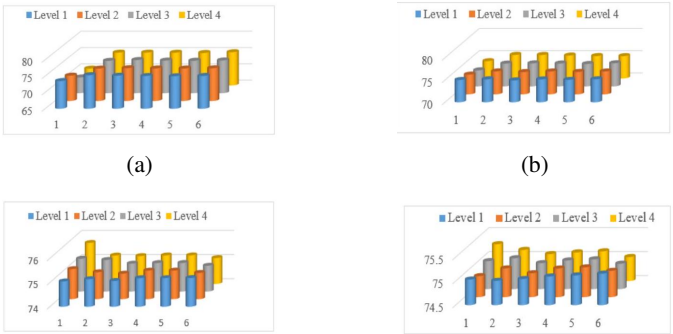

(a) (b)

(c) (d)

Fig. 4: OCL values after segmentation for (a) Haar, (b) db2, (c) sym4 and (d) boir2.6

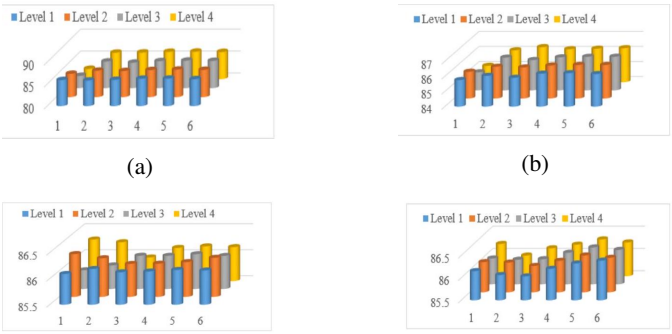

(a) (b)

(c) (d)

Fig. 5: OCL values after ridge structure enhancement for (a) Haar, (b) db2 ,(c) sym4 and (d) boir2.6

research endeavor, consistent and superior outcomes have been consistently observed using the proposed method in conjunction with the bior2.6 wavelet filter.

- Significant improvements were observed in the OCL values, with a remarkable increase of 11% attributed to the segmentation process. This notable enhancement can be attributed to the application of the ridge structure enhancement technique, which results in sharper and more prominent fingerprint ridges and valleys. The refinement achieved through this process ensures greater precision and prominence, leading to the observed improvement in OCL values.

XI. Conclusion and Future Work

In this study, a robust approach was developed by combining the wavelet-based technique for speckle noise removal in OCT latent fingerprint images with morphological segmentation and ridge structure enhancement. The effectiveness of this combination is clearly demonstrated by the results obtained from the OCL analysis. Moving forward, the next steps involve the extraction of minutiae points and fingerprint matching, which will further advance the application of this technique.

References

[1] Iwasokun Gabriel Babatunde, Akinyokun Oluwole Charles, and Olabode Olatunbosun. Uniformity level approach to fingerprint ridge frequency estimation. *International Journal of Computer Applications*, 62(22), 2013.

[2] Sarat C Dass and Anil K Jain. Fingerprint classification using orientation field flow curves. In *ICVGIP*, pages 650–655, 2004.

[3] John Daugman and Cathryn Downing. Gabor wavelets for statistical pattern recognition. In *The handbook of brain theory and neural networks*, pages 414–420. 1998.

[4] Shoba Dyre and CP Sumathi. Reliable orientation field estimation of fingerprint based on adaptive neighborhood analysis. *ICTACT Journal on Image & Video Processing*, 7(3), 2017.

[5] Mamdouh F Fahmy and MA Thabet. A fingerprint segmentation technique based on morphological processing. In *IEEE International Symposium on Signal Processing and Information Technology*, pages 000215–000220. IEEE, 2013.

[6] R Fisher, S Perkins, A Walker, and E Wolfart. Adaptive thresholding.

[7] RC Gonzalez, RE Woods, and SL Eddins. Digital image processing using matlab, pearson education india, 2004.

[8] Ross Philip Holder and Jules-Raymond Tapamo. Using facial expression recognition for crowd monitoring. In *Pacific-Rim Symposium on Image and Video Technology*, pages 463–476. Springer, 2017.

[9] Lin Hong, Yifei Wan, and Anil Jain. Fingerprint image enhancement: Algorithm and performance evaluation. *IEEE transactions on pattern analysis and machine intelligence*, 20(8):777–789, 1998.

[10] Michael Kass and Andrew Witkin. Analyzing oriented patterns. *Computer vision, graphics, and image processing*, 37(3):362–385, 1987.

[11] Nontokozo Portia Khanyile. *Fingerprint identification using distributed computing*. PhD thesis, 2012.

[12] M Kocevar, S Klampfer, A Chowdhury, and Z Kacic. Low-quality fingerprint image enhancement on the basis of oriented diffusion and ridge compensation. *Elektronika Ir Elektrotechnika*, 20(8):49–54, 2014.

[13] Ravinder Kumar, Pravin Chandra, and M Hanmandlu. Fingerprint singular point detection using orientation field reliability. In *Advanced Materials Research*, volume 403, pages 4499–4506. Trans Tech Publ, 2012.

[14] E Jebamalar Leavline, S Sutha, and D Asir Antony Gnana Singh. Wavelet domain shrinkage methods for noise removal in images: A compendium. *International Journal of Computer Applications*, 33(10):28–32, 2011.

[15] Sboniso Sifiso Mgaga, Jules-Raymond Tapamo, and Nontokozo Portia Khanyile. Optical coherence tomography latent fingerprint image denoising. In *International Symposium on Visual Computing*, pages 694–705. Springer, 2020.

[16] Rohan Nimkar and Agya Mishra. Fingerprint segmentation algorithms: A literature review. *International Journal of Computer Applications*, 95(5), 2014.

[17] Thai Raymond. Fingerprint image enhancement and minutiae extraction. *Report in the School of Computer Science and Software Engineering*, 2003.

[18] Sujata Saini and Komal Arora. A study analysis on the different image segmentation techniques. *International Journal of Information & Computation Technology*, 4(14):1445–1452, 2014.

[19] Pierre Soille. Erosion and dilation. In *Morphological Image Analysis*, pages 63–103. Springer, 2004.

[20] M James Stephen, Prasad Reddy, et al. Enhancing fingerprint image through ridge orientation with neural network approach and ternarization for effective minutiae extraction. *International Journal of Machine Learning and Computing*, 2(4):397, 2012.

[21] Lukasz Wieclaw. Fingerprint orientation field enhancement. In *Computer Recognition Systems 4*, pages 33–40. Springer, 2011.

[22] Lukasz Wieclaw. Gradient based fingerprint orientation field estimation. *Journal of Medical Informatics & Technologies*, 22, 2013.

[23] Fei Xiao and Yungang Zhang. A comparative study on thresholding methods in wavelet-based image denoising. *Procedia Engineering*, 15:3998–4003, 2011.

[24] David Zhang, Feng Liu, Qijun Zhao, Guangming Lu, and Nan Luo. Selecting a reference high resolution for fingerprint recognition using minutiae and pores. *IEEE Transactions on Instrumentation and Measurement*, 60(3):863–871, 2010.